

## Material descriptors for morphotropic phase boundary curvature in lead-free piezoelectrics

Dezhen Xue, Prasanna V. Balachandran, Haijun Wu, Ruihao Yuan, Yumei Zhou, Xiangdong Ding, Jun Sun, and Turab Lookman

Citation: *Appl. Phys. Lett.* **111**, 032907 (2017);

View online: <https://doi.org/10.1063/1.4990955>

View Table of Contents: <http://aip.scitation.org/toc/apl/111/3>

Published by the [American Institute of Physics](#)

---

### Articles you may be interested in

[Ferroelectric, elastic, piezoelectric, and dielectric properties of  \$\text{Ba}\(\text{Ti}\_{0.7}\text{Zr}\_{0.3}\)\text{O}\_3\text{-x}\(\text{Ba}\_{0.82}\text{Ca}\_{0.18}\)\text{TiO}\_3\$  Pb-free ceramics](#)

*Journal of Applied Physics* **122**, 044105 (2017); 10.1063/1.4996353

[Ferroelectric, pyroelectric, and piezoelectric properties of a photovoltaic perovskite oxide](#)

*Applied Physics Letters* **110**, 063903 (2017); 10.1063/1.4974735

[Enhanced energy storage density by inducing defect dipoles in lead free relaxor ferroelectric  \$\text{BaTiO}\_3\$ -based ceramics](#)

*Applied Physics Letters* **110**, 132902 (2017); 10.1063/1.4979467

[Thermally stable electrostrains of morphotropic  \$0.875\text{NaNbO}\_3\text{-0.1BaTiO}\_3\text{-0.025CaZrO}\_3\$  lead-free piezoelectric ceramics](#)

*Applied Physics Letters* **110**, 112903 (2017); 10.1063/1.4978694

[Pressure driven depolarization behavior of  \$\text{Bi}\_{0.5}\text{Na}\_{0.5}\text{TiO}\_3\$  based lead-free ceramics](#)

*Applied Physics Letters* **110**, 212901 (2017); 10.1063/1.4984088

[Correlation between structure and Rayleigh parameters in the lead-free piezoceramic  \$\(1\text{-x}\)\text{Ba}\(\text{Ti}\_{0.88}\text{Sn}\_{0.12}\)\text{O}\_3\text{-x}\(\text{Ba}\_{0.7}\text{Ca}\_{0.3}\)\text{TiO}\_3\$](#)

*Journal of Applied Physics* **122**, 034101 (2017); 10.1063/1.4990119

---

**Scilight**

Sharp, quick summaries **illuminating**  
the latest physics research

Sign up for **FREE!**



## Material descriptors for morphotropic phase boundary curvature in lead-free piezoelectrics

Dezhen Xue,<sup>1,2,a)</sup> Prasanna V. Balachandran,<sup>2</sup> Haijun Wu,<sup>3</sup> Ruihao Yuan,<sup>1</sup> Yumei Zhou,<sup>1</sup> Xiangdong Ding,<sup>1</sup> Jun Sun,<sup>1</sup> and Turab Lookman<sup>2,b)</sup>

<sup>1</sup>State Key Laboratory for Mechanical Behavior of Materials, Xi'an Jiaotong University, Xi'an 710049, China

<sup>2</sup>Theoretical Division, Los Alamos National Laboratory, Los Alamos, New Mexico 87545, USA

<sup>3</sup>Department of Materials Science and Engineering, National University of Singapore, 117575 Singapore

(Received 22 January 2017; accepted 16 June 2017; published online 20 July 2017)

An important aspect of searching for alternatives to the current piezoelectric workhorse PZT ( $\text{PbZr}_x\text{Ti}_{1-x}\text{O}_3$ ) is to establish a vertical morphotropic phase boundary (MPB) in the composition-temperature phase diagram. However, the MPBs in most lead-free piezoelectrics, especially the  $\text{BaTiO}_3$ -based piezoelectrics, are not as vertical as that of PZT, resulting in serious temperature dependence of piezoelectric and dielectric properties. We investigate the dependence of the verticality of the MPB on polarization and strain related design descriptors in  $\text{BaTiO}_3$ -based and Pb-based systems. We find that the slope of the MPB decreases monotonically with the unit cell volume ratio of the tetragonal (T) and rhombohedral (R) ends; however, it increases with the ionic displacement ratio of the two ends. As the above two descriptors are not straight forward to access as *a priori* information, two parameters that relate to the atomic size and effective nuclear charge are introduced to enable an effective search for a desired MPB slope. Our study thus provides potential selection rules for developing Pb-free piezoelectrics with high temperature reliability. *Published by AIP Publishing.* [<http://dx.doi.org/10.1063/1.4990955>]

The electromechanical coupling of piezoelectric materials leads to many applications ranging from sensors to actuators.<sup>1,2</sup> The PZT [lead zirconate titanate,  $\text{Pb}(\text{Ti}_{1-x}\text{Zr}_x)\text{O}_3$ ] family has served as the prototype of piezoelectric materials as its piezoelectric response attains both high value and good temperature insensitivity.<sup>3</sup> Nevertheless, PZT is currently facing global restrictions due to  $\text{Pb}^{2+}$  toxicity, and therefore, there is urgent demand for Pb-free alternatives.<sup>4-6</sup>

To enhance the piezoelectricity of Pb-free alternatives so that it approaches that of PZT, it is important to establish a phase boundary between two ferroelectric phases in the composition-temperature phase diagram.<sup>7</sup> When a compound is placed in the vicinity of the ferroelectric phase boundary (at a certain composition and temperature, usually room temperature), the polarization and/or structure instabilities give rise to a strong piezoelectric response.<sup>4-7</sup> However, this only ensures high piezoelectricity at a certain temperature. To maintain high temperature reliability, i.e., large response over a wide temperature range, the phase boundary should be close to vertical in the temperature-composition phase diagram.<sup>6,8</sup> The phase boundary for PZT, known as the morphotropic phase boundary (MPB), certainly approaches being vertical.<sup>3,9</sup> MPB composition,  $x = 0.48$ , PZT remains in the MPB region in spite of temperature variations, giving rise to excellent temperature reliability in its piezoelectric properties.<sup>10,11</sup> Strictly, the MPB region includes orthorhombic or monoclinic phases identified by diffraction or microscopy studies. In contrast, the measurement data in this work do not resolve these phases, and thus, we treat the MPB as a single boundary.

Although several Pb-free substitutes can already compete with PZT in their  $d_{33}$  (with  $d_{33} = 500\text{--}600$  pC/N) values, almost all of them have inferior temperature reliability compared to PZT.<sup>7,12-16</sup> The reason is that the phase boundaries in Pb-free systems are tilted or curved in their composition-temperature phase diagram, especially for the  $\text{BaTiO}_3$ -based systems.<sup>7,17-19</sup> The recently reported  $\text{Ba}(\text{Zr}_{0.2}\text{Ti}_{0.8})\text{O}_3 - x(\text{Ba}_{0.7}\text{Ca}_{0.3})\text{TiO}_3$  (BZT- $x$ BCT) system possesses a tilted/curved phase boundary.<sup>7,20</sup> As the temperature deviates from the phase boundary, the compound is brought away from the instabilities controlling response, and consequently, the magnitude of its response drops. Therefore, a serious obstacle for Pb-free substitutions is the temperature sensitive behavior, which originates from a tilted/curved phase boundary in the composition-temperature phase diagram. Nevertheless, fundamental variables or *descriptors* that determine the “verticality” of the MPB first need to be established, that is, we lack a design rule for vertical MPBs.

Crystal chemical descriptors can permit accurate predictions of properties such as ionic displacement,<sup>22</sup> the phase transition temperature,<sup>23,24</sup> and tetragonality.<sup>25</sup> Phenomenological models and scatter plots have been used to capture trends in experimental data, including those for solid solutions. Statistical models have also been formulated to predict compounds with targeted properties, such as high Curie temperatures.<sup>26</sup> It has already been shown that an MPB in the composition-temperature phase diagram can be established by combining a compound undergoing a cubic (C) to tetragonal (T) phase transition at one end with another undergoing a cubic (C) to rhombohedral (R) phase transition at the other end.<sup>7</sup> For example, the combination of  $\text{Ba}(\text{Zr}_{0.2}\text{Ti}_{0.8})\text{O}_3$  at the R-end with  $(\text{Ba}_{0.7}\text{Ca}_{0.3})\text{TiO}_3$  at the T-end leads to the discovery of the Pb-free systems with good piezoelectric performance.<sup>17-20</sup>

<sup>a)</sup>Electronic mail: xuedezhen@xjtu.edu.cn

<sup>b)</sup>Electronic mail: txl@lanl.gov

These phase diagrams with different chemistries at their two ends are characterized by phase boundaries with varying degrees of “verticality.” Therefore, knowledge of how the phase boundary changes with different dopants and their concentrations at the two ends of the phase diagram offers an opportunity to probe the descriptors that determine the verticality of the phase boundary. Our goal in this work is to identify the descriptors for the shape of the MPB in lead-free piezoelectrics.

We focused on the  $BaTiO_3$ -based systems and combined the T-end and R-end compounds with different phase transitions ( $C \rightarrow T$  or  $C \rightarrow R$ ) to establish an MPB in the pseudo-binary phase diagram. The  $Ca^{2+}$  doped  $BaTiO_3$  was chosen as the T end, and  $Sn^{4+}$ ,  $Zr^{4+}$ ,  $Hf^{4+}$  doped  $BaTiO_3$  was chosen as the R end. We explored 20  $BaTiO_3$  based systems and 3 Pb-based systems.<sup>3,9,27,28</sup> Table I in [supplementary material](#) lists the data for systems used in the present study. We note that because of differences between the phase diagrams determined by different investigators and methods, four of the 20  $BaTiO_3$  based systems have been reported by our group<sup>17–20</sup> and the rest were fabricated in this study using the same processing conditions to minimize variability due to processing and microstructural effects. Within each phase diagram, the MPB is a function of the transition temperature  $\tau$  and concentration  $x$  (relative fraction of two ends in the binary composition-temperature phase diagrams). Figure 1(a) shows a typical experimental phase diagram with an MPB between tetragonal and rhombohedral ends and the three ways we defined the “verticality” of the MPB. The linear slope  $\alpha$ , the polynomial coefficient  $\alpha_2$ , and the composition interval  $\Delta x$  represent the degree of curvature or shape of the phase boundary and they are linearly correlated, as shown in Fig. 1(b). We chose the linear slope  $\alpha$  for simplicity.

As piezoelectrics are electromechanically coupled, polarization and strain serve as the primary and secondary order parameters. Thus, we considered parameters related to strain and polarization for both ends of the phase diagram. The two ends of the phase diagram usually possess differing unit cell volumes, as the dopants and their concentrations are different. We take the ratio of the unit cell volumes at the two ends ( $r_V$ ) as our descriptor related to strain. This is given by  $r_V = \frac{V_T}{V_R}$ , where  $V_T$  and  $V_R$  are the unit cell volumes

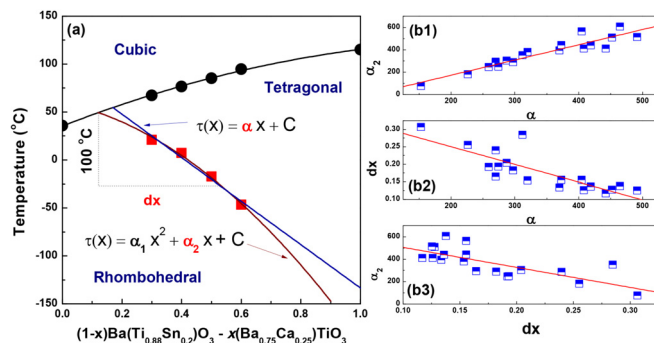


FIG. 1. (a) Definitions of the property. These include a linear fit,  $\tau(x) = \alpha x + C$ , a quadratic fit,  $\tau(x) = \alpha_1 x^2 + \alpha_2 x + C$ , and a linear composition interval  $\Delta x$  from the phase boundary at room temperature (RT) to a point 100 °C below. (b) The three definitions ( $\alpha$ ,  $\alpha_2$ , and  $\Delta x$ ) of the property are linearly correlated.

of the T- and R-ends, respectively. For our R-end with  $Ba(Ti_{1-n}Zr_n)O_3$  and  $Ba(Ti_{1-n}Sn_n)O_3$ , we utilized Vegard’s law (effective lattice constant,  $a$  is linearly dependent on the dopant concentration) to obtain the unit cell volume for different dopant concentrations. This gives  $a = 4.0046 + 0.187n$  for  $Ba(Ti_{1-n}Zr_n)O_3$  and  $a = 4.0046 + 0.11n$  for  $Ba(Ti_{1-n}Sn_n)O_3$ .<sup>29,30</sup> Similarly, the effective lattice parameter for  $(Ba_{1-m}Ca_m)TiO_3$ , the T-end, is given by  $a = 4.00999 - 0.148m$ , if  $m$  is lower than a threshold of 0.35, above which the lattice parameters are almost constant.<sup>31</sup> The unit cell volume for  $Ba(Ti_{0.8}Hf_{0.2})O_3$  and Pb-based systems are taken from the literature.<sup>32,33</sup> Note that Vegard’s law is usually valid for systems containing single dopants but not for multi-component systems; thus, the volume of the two ends is actually not easy to obtain. The calculated  $r_V$  values for  $BaTiO_3$  based systems in this study are within the 0.8836–0.9529 range, whereas those for Pb-based systems are within 0.9261–0.9723.

Figure 2(a) illustrates the significant variation in the slope  $\alpha$  with the descriptor  $r_V$ . Two distinct trends are observed in  $BaTiO_3$ -based and Pb-based systems. In both cases, the slope,  $\alpha$ , increases monotonically with increasing  $r_V$ , but the Pb-based system has a slope almost 7 times larger. As shown in Fig. 2(a), for  $BaTiO_3$ -based systems, it is difficult to generate a similar vertical phase boundary as PZT. For example, even if one can make a  $BaTiO_3$  system with the same  $r_V$  as

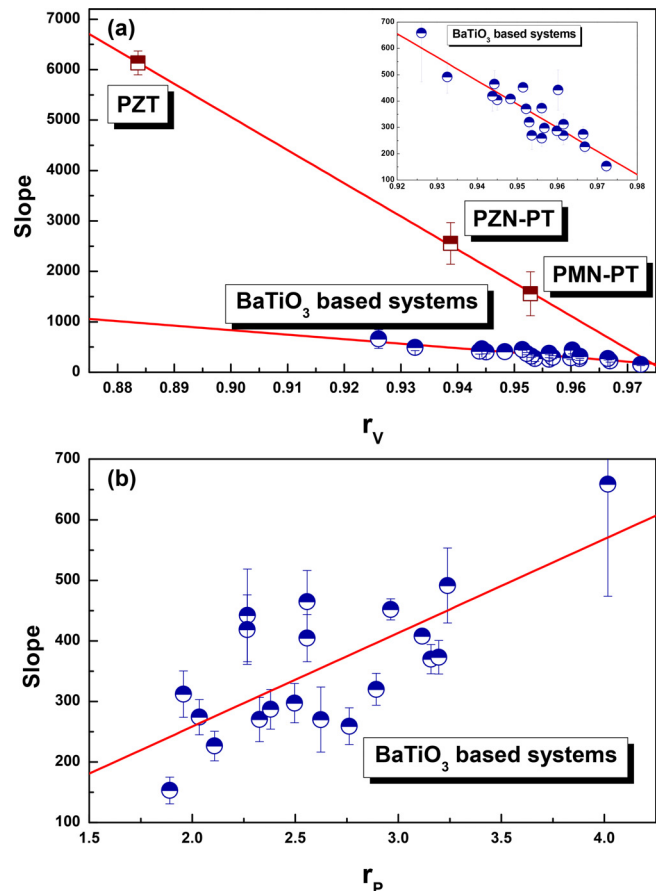


FIG. 2. The dependence of the slope ( $\alpha$ ) of the MPB as a function of (a) the descriptor  $r_V$  (the ratio of the unit cell volume at the two ends) and (b) the descriptor  $r_P$  (the ratio of ionic displacements at the two ends). Inset magnifies the region of  $BaTiO_3$  based system. The error bar indicates the error of linearly fitting to the phase boundary.

PZT, the expected slope is only 980, 6 times lower than that of PZT. Such distinct behavior is likely connected to the presence of transitions to lower symmetry phases in  $BaTiO_3$ , and the absence of such transitions in  $PbTiO_3$ . According to Fig. 2(a), it appears that the linear dependence for both systems converges at the point (1,0), indicating that when the unit cell volumes are the same for the two ends, there may not exist an MPB line in either system. Therefore, Fig. 2(a) suggests that the larger the unit cell volume difference is, the more vertical is the MPB.

As for the ratio of unit cell volumes, we anticipate that the polarization difference between the two ends of the phase diagram plays a similar role in determining the slope of the MPB. It is known that ionic displacements correlate strongly with the polarization for ferroelectric perovskites (although for more quantitative treatment of polarization, it is important to include the electronic contribution term in addition to the ionic term), and the ferroelectric transition temperature,  $T_c$ , in certain systems has been shown to increase quadratically with the displacements.<sup>34,35</sup>

Here, we define displacements in terms of the symmetry-adapted distortion-modes associated with the Cubic (C) to T and C to R phase transitions and these are used to calculate  $D^{A_T}$  and  $D^{B_R}$ , respectively,<sup>21</sup> (see the [supplementary material](#) for details). Since, we consider solid solutions in this work,  $D_T^A$  and  $D_T^B$  are then uniquely described as a mole fraction of these mode amplitudes that are calculated for the pure compounds. We thus utilized the ratio of displacements at the two ends ( $r_P$ ) as our descriptor related to polarization, given by  $r_P = \frac{D_T^A}{D_T^B}$ , where  $D_T^A$  and  $D_T^B$  are the displacements of the solid solutions at the T and R-ends, respectively. The calculated  $r_P$  values for  $BaTiO_3$  based systems in this study are within the range of 1.8906–4.0163.

Figure 2(b) shows how  $\alpha$  increases with  $r_P$  in  $BaTiO_3$ -based systems. This behavior is similar to that for  $r_V$ , but the correlation is not strong. The  $\mathfrak{R}^2$  values for  $r_V$  and  $r_P$  are 0.7754 and 0.5209, respectively. The weak correlation between slope of MPB and  $r_P$  indicates that only the ionic contribution to the polarization (as we did for  $r_P$ ) is not adequate to determine the slope of the MPB. The electronic contribution to the polarization should also play an important role. Nevertheless, it is clear that the larger the polarization difference, the more vertical is the MPB.

The dependence of the slope of the MPB on unit cell volume ratio ( $r_V$ ) and ionic displacement ratio ( $r_P$ ) shown in Fig. 2 offers simple guidelines for vertical MPBs. That is, a vertical MPB can be achieved by combining two ends with a large difference in the unit cell volume and ionic displacement. Statistical regression based on the two descriptors ( $r_V$  and  $r_P$ ) can provide good predictions for the slope, as will be shown in the last paragraph. However, the use of the two descriptors ( $r_V$  and  $r_P$ ) to design piezoelectric systems requires information of lattice parameters and ionic displacements as *a priori* knowledge. In most cases, this requires diffraction measurements or density functional theory (DFT) calculations, and therefore is not easy to obtain in advance. Thus, simple descriptors that are easily accessible are more meaningful for materials design. We therefore introduce two descriptors which correlate well with  $r_V$  and  $r_P$ , respectively.

We define a parameter which is determined from lattice parameters to replace  $r_V$ . It has already been shown that the ionic size can be used to predict bond lengths. For example, Shannon and Prewitt assigned a particular ionic size and obtained the bond length by adding the ionic radii of the two atoms.<sup>36–38</sup> In the perovskite  $ABO_3$  structure, in order to characterize the A-O and B-O sublattice competition, the ionic size is also utilized to define the so-called tolerance factor  $t$  as  $t = (R_A + R_O)/\sqrt{2}(R_B + R_O)$ , where  $R_A$ ,  $R_B$ , and  $R_O$  are ionic radii of the  $A^{2+}$ ,  $B^{4+}$ , and  $O^{2-}$  ions, respectively.<sup>39</sup> In the case of  $r_V$ , the volumes at the two ends are related to the lattice parameters, which in turn are related to the ionic bond lengths. Thus, we can replace  $r_V$  by the bond length difference at the two ends, which in turn is related to the ionic radii. An additional consideration is that the T-end is always obtained by doping  $BaTiO_3$  at the A site and the R-end is obtained by doping  $BaTiO_3$  at the B site. We consider this doping to give the dominant contribution. Therefore, we define the ratio of ionic radii at the two ends,  $r_R$ , as our descriptor that replaces  $r_V$ . This is given by  $r_R = \frac{R_T^A}{R_R^B}$ , where  $R_T^A$  is the ionic radii of the A site ion at the T-end, and  $R_R^B$  is the ionic radii of the B site ion at the R-end. The ionic radii data are taken from the literature<sup>37</sup> and the ionic radii for the solid solution were determined from the mole fraction of the ions.

Limiting ourselves to  $BaTiO_3$ -based systems, Fig. 3 (first and second columns) shows that  $r_V$  and  $r_R$  are positively correlated with a correlation coefficient of about 0.91. We plotted the slope,  $\alpha$ , in both Pb-based and  $BaTiO_3$ -based systems as a function of the parameter  $r_R$  in Fig. 4(a). Again, two classes of behavior can be observed corresponding to the  $BaTiO_3$ -based and Pb-based systems, respectively. In both cases, the slope  $\alpha$  increases monotonically upon increasing  $r_R$ , similar to  $r_V$ . The slope of the Pb-based system is 7 times larger than  $BaTiO_3$ . Thus,  $r_R$  and  $r_V$  are closely correlated and  $r_R$  can replace  $r_V$  as a design descriptor.

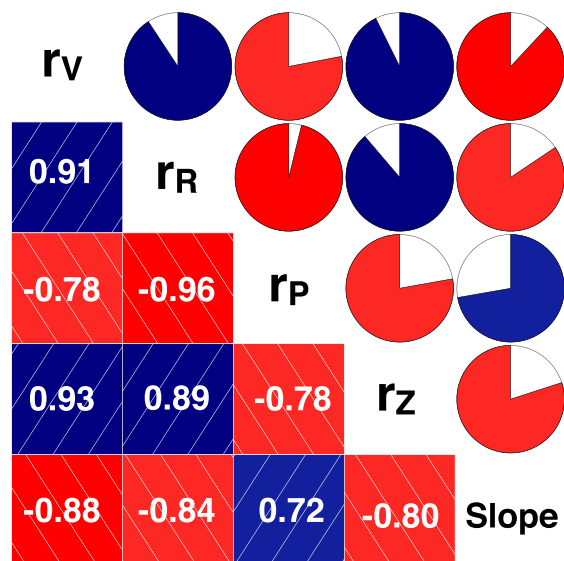


FIG. 3. The correlation map for slope ( $\alpha$ ) of the phase boundary and four different descriptors defined in the present study. The red color indicates positive correlation while the blue color indicates negative correlation. The colored pies show the extent of correlation and the actual values are shown in the lower half of the figure.



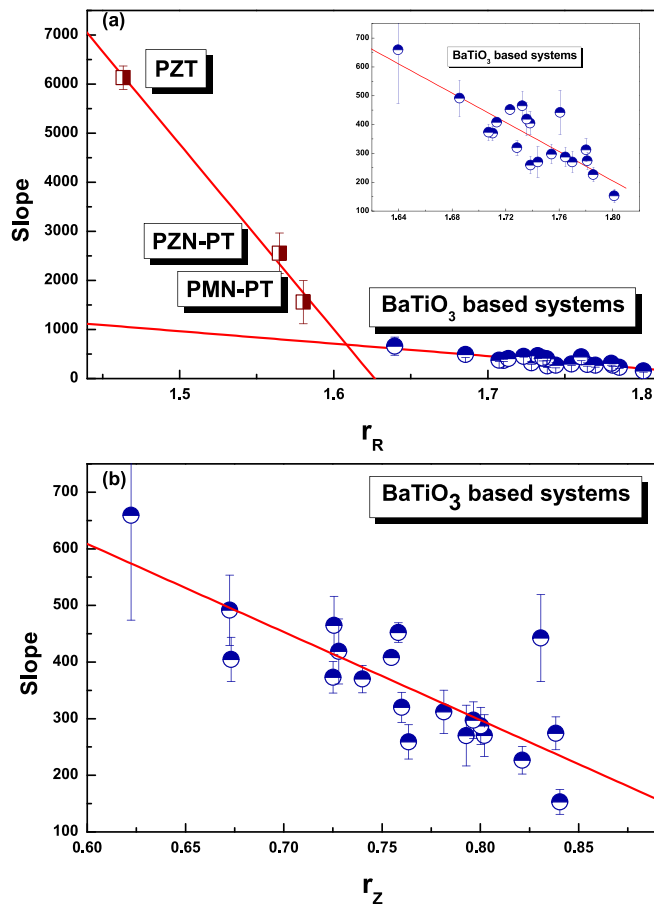


FIG. 4. The dependence of the slope ( $\alpha$ ) of the MPB as a function of (a) the descriptor  $r_R$  (the ratio of the atomic radii at the two ends) and (b) the descriptor  $r_Z$  (the ratio of effective nuclear charge at the two ends). The inset magnifies the region of  $BaTiO_3$  based system. The error bar indicates the error of linearly fitting to the phase boundary.

We can similarly define an easily accessible descriptor that plays the same role as the ionic displacement ratio,  $r_P$ , in determining the slope of the MPB. The  $r_P$  is from the ionic displacements at the two ends, which are closely related to the polarization strength of the cations in the perovskite structure. A so-called effective ionic potential  $\phi$  has been considered as a measure of the degree of polarization of the cations.<sup>40,41</sup> It is defined as  $\phi = Z^*/r$ , where the effective nuclear charge  $Z^* = Z - \Sigma s$ ,  $Z$  is the atomic number,  $\Sigma s$  is the shield factor, and  $r$  is the ion radius.<sup>40,41</sup> Therefore, the degree of polarization can be considered to be proportional

to the effective nuclear charge  $Z^*$ .<sup>42</sup> We considered the difference in the effective nuclear charge  $Z^*$  between the T and R ends to play the same role as the ionic displacement ratio,  $r_P$ . We similarly used the effective nuclear charge at the A site of the T-end and that at the B site of the R-end for  $r_P$ . Therefore, we define the ratio of ionic radii between the two ends,  $r_Z$ , as our descriptor related to polarization, and it is given by  $r_Z = \frac{Z_T^A}{Z_R^B}$ , where  $Z_T^A$  and  $Z_R^B$  are the effective nuclear charge of the A site ion at the T-end and the effective nuclear charge of the B site ion at the R-end. The effective nuclear charge of the solid solution was determined from the mole fraction of ions.

Within the  $BaTiO_3$ -based systems, Fig. 3 (third and fourth columns) shows that  $r_Z$  and  $r_P$  are negatively correlated and the correlation coefficient is about 0.78. We plotted the slope,  $\alpha$ , in both  $Pb$ - and  $BaTiO_3$ -based systems as a function of the parameter  $r_Z$  in Fig. 4(b). In  $BaTiO_3$ -based systems,  $\alpha$  increases monotonically with increasing  $r_Z$ , similar to  $r_P$ . The correlation between  $r_Z$  and  $\alpha$  is even better than that between  $\alpha$  and  $r_P$  with a coefficient of 0.72, as shown in Fig. 3. However, the  $Pb$ -based system does not have such a linear correlation, and a better descriptor that can capture the polarization behavior is still needed. Thus, in summary,  $r_R$  and  $r_V$  are closely correlated and  $r_R$  can replace  $r_V$  as a design descriptor.

With the above selected descriptors, we were able to model the slope,  $\alpha$ , to predict unexplored pseudo-binary phase diagrams. A linear regression model based on the descriptors works very well. We compared three linear models: (i) using all four descriptors  $r_V$ ,  $r_P$ ,  $r_R$ , and  $r_Z$ ; (ii) using  $r_V$  and  $r_P$ , and (iii) using  $r_R$  and  $r_Z$ . We used the method of “bootstrap resampling” to create a large number of samples characteristic of the population. We first constructed 1000 “bootstrap” samples and developed 1000 different linear models from our 20 data points (phase diagrams). With predictions from the 1000 different linear models for all the data points, we estimated the mean and standard deviation of the training set.

Figure 5 compares the results of our three models. It is clear that our model using all four descriptors outperforms the other two, as shown in Fig. 5(a) with  $R^2 = 0.834$ . Figure 5(b) shows the second best model, using  $r_V$  and  $r_P$  with  $R^2 = 0.779$ . However, these models have the limitation that  $r_V$  and  $r_P$  are not easy to obtain for unexplored or un-synthesized systems.

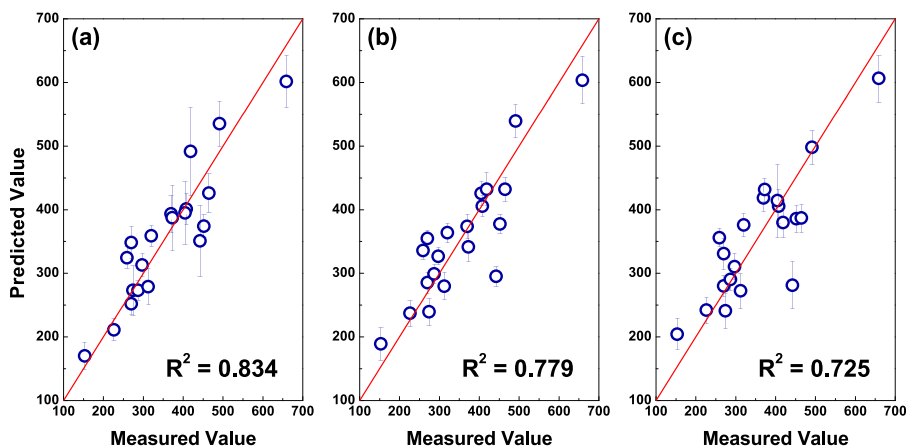


FIG. 5. Linear regression models, (a) using all four descriptors  $r_V$ ,  $r_P$ ,  $r_R$ , and  $r_Z$ ; (b) with  $r_V$  and  $r_P$ , and (c) using  $r_R$  and  $r_Z$ . Error bars are estimated from 1000 bootstrap samples.

Figure 5(c) shows the performance of the model with  $r_R$  and  $r_Z$ . The model is fairly good and without overfitting. Therefore, it can be used to predict the slope of the MPB for any combination of dopants at the two ends.

As noted previously, the MPBs in  $BaTiO_3$  based systems are not “morphotropic” in the sense that there is no abrupt composition induced transition between T and R phases and an intermediate phase (orthorhombic or monoclinic phase) always bridges the T and R phases. Thus, a method to further improve the predictive model is to identify descriptors that capture the presence of the intermediate phase.

In summary, from our study of correlations, we find that the descriptors  $r_V$  and  $r_P$  have the most influence on the slope or verticality of the MPB in both  $BaTiO_3$  based and  $Pb$ -based systems. The slope  $\alpha$  is found to decrease monotonically with the unit cell volume ratio ( $r_V$ ) and the ionic displacement ratio ( $r_P$ ) of the tetragonal (T) and rhombohedral (R) ends ( $r_V$ ). As  $r_V$  and  $r_P$  are not easily accessible, especially for multi-component systems, we have proposed two descriptors to represent them. A descriptor defined by the ratio of ionic radii between the two ends replaces  $r_V$ , while a descriptor defined by the ratio of effective nuclear charge between two ends substitutes  $r_P$ . Based on these descriptors, machine learning algorithms can be employed to predict the slope of the MPB for unexplored systems. Our study provides a potential selection rule for developing Pb-free piezoelectrics with high temperature reliability.

See [supplementary material](#) for the definition of the ionic displacement and the training dataset.

The authors gratefully acknowledge the support of the National Natural Science Foundation of China (Grant Nos. 51302209, 51671157, 51571156, 51621063, 51431007, and 51320105014).

<sup>1</sup>K. Uchino, *Ferroelectric Devices* (CRC Press, 2009), p. 367.

<sup>2</sup>*Handbook of Advanced Dielectric, Piezoelectric and Ferroelectric Materials: Synthesis, Properties and Applications*, edited by Z. Ye (Woodhead Publishing, 2008), p. 1096.

<sup>3</sup>*Piezoelectric Ceramics*, edited by B. Jaffe, W. R. Cook, and H. Jaffe (Academic Press, 1971), p. 328.

<sup>4</sup>T. R. Shrout and S. J. Zhang, *J. Electroceram.* **19**, 113–126 (2007).

<sup>5</sup>J. Rödel, K. G. Webber, R. Dittmer, W. Jo, M. Kimura, and D. Damjanovic, *J. Eur. Ceram. Soc.* **35**, 1659–1681 (2015).

<sup>6</sup>J. Rödel, W. Jo, K. T. Seifert, E.-M. Anton, T. Granzow, and D. Damjanovic, *J. Am. Ceram. Soc.* **92**, 1153–1177 (2009).

<sup>7</sup>W. Liu and X. Ren, *Phys. Rev. Lett.* **103**, 257602 (2009).

<sup>8</sup>D. Xue, P. V. Balachandran, R. Yuan, T. Hu, X. Qian, E. Dougherty, and T. Lookman, *PNAS* **113**, 13301–13306 (2016).

<sup>9</sup>A. Bouzid, E. Bourim, M. Gabbay, and G. Fantozzi, *J. Eur. Ceram. Soc.* **25**, 3213–3221 (2005).

<sup>10</sup>R. Georges Sabat, B. K. Mukherjee, W. Ren, and G. Yang, *J. Appl. Phys.* **101**, 064111 (2007).

<sup>11</sup>A. A. Heitmann and G. A. Rossetti, *J. Am. Ceram. Soc.* **97**, 1661–1685 (2014).

<sup>12</sup>Y. Saito, H. Takao, T. Tani, T. Nonoyama, K. Takatori, T. Homma, T. Nagaya, and M. Nakamura, *Nature* **432**, 84–87 (2004).

<sup>13</sup>X. Wang, J. Wu, D. Xiao, J. Zhu, X. Cheng, T. Zheng, B. Zhang, X. Lou, and X. Wang, *J. Am. Chem. Soc.* **136**, 2905–2910 (2014).

<sup>14</sup>J. Wu, D. Xiao, and J. Zhu, *Chem. Rev.* **115**, 2559–2595 (2015).

<sup>15</sup>J. Zylberberg, A. A. Belik, E. Takayama-Muromachi, and Z.-G. Ye, *Chem. Mater.* **19**, 6385–6390 (2007).

<sup>16</sup>B. Wu, H. Wu, J. Wu, D. Xiao, J. Zhu, and S. J. Pennycook, *J. Am. Chem. Soc.* **138**, 15459–15464 (2016).

<sup>17</sup>D. Xue, Y. Zhou, H. Bao, J. Gao, C. Zhou, and X. Ren, *Appl. Phys. Lett.* **99**, 122901 (2011).

<sup>18</sup>H. Bao, C. Zhou, D. Xue, J. Gao, and X. Ren, *J. Phys. D: Appl. Phys.* **43**, 465401 (2010).

<sup>19</sup>C. Zhou, W. Liu, D. Xue, X. Ren, H. Bao, J. Gao, and L. Zhang, *Appl. Phys. Lett.* **100**, 222910 (2012).

<sup>20</sup>D. Xue, Y. Zhou, H. Bao, C. Zhou, J. Gao, and X. Ren, *J. Appl. Phys.* **109**, 054110 (2011).

<sup>21</sup>P. V. Balachandran, D. Xue, and T. Lookman, *Phys. Rev. B* **93**, 144111 (2016).

<sup>22</sup>I. Grinberg and A. M. Rappe, *Phys. Rev. Lett.* **98**, 037603 (2007).

<sup>23</sup>W.-C. Lee, C.-Y. Huang, L.-K. Tsao, and Y.-C. Wu, *J. Eur. Ceram. Soc.* **29**, 1443 (2009).

<sup>24</sup>R. E. Eitel, C. A. Randall, T. R. Shrout, P. W. Rehrig, W. Hackenberger, and S.-E. Park, *Jpn. J. Appl. Phys., Part 1* **40**, 5999 (2001).

<sup>25</sup>M. R. Suchomel and P. K. Davies, *Appl. Phys. Lett.* **86**, 262905 (2005).

<sup>26</sup>P. V. Balachandran, S. R. Broderick, and K. Rajan, *Proc. R. Soc. London A* **467**, 2271 (2011).

<sup>27</sup>T. R. Shrout, Z. P. Chang, N. Kim, and S. Markgraf, *Ferroelectr. Lett. Sect.* **12**, 63–69 (1990).

<sup>28</sup>D. Cox, B. Noheda, G. Shirane, Y. Uesu, K. Fujishiro, and Y. Yamada, *Appl. Phys. Lett.* **79**, 400–402 (2001).

<sup>29</sup>M. McQuarrie and F. W. Behnke, *J. Am. Ceram. Soc.* **37**, 539–543 (1954).

<sup>30</sup>X. Wei and X. Yao, *Mater. Sci. Eng., B* **137**, 184–188 (2007).

<sup>31</sup>G. Durst, M. Grotenhuis, and A. Barkow, *J. Am. Ceram. Soc.* **33**, 133–139 (1950).

<sup>32</sup>W. H. Payne and V. J. Tennery, *J. Am. Ceram. Soc.* **48**, 413–417 (1965).

<sup>33</sup>*Landolt-Bornstein—Group III Condensed Matter 36A1 (Oxides)*, edited by Y. Shiozaki, E. Nakamura, and T. Mitsui (SpringerMaterials, 2001).

<sup>34</sup>S. C. Abrahams, S. K. Kurtz, and P. B. Jamieson, *Phys. Rev.* **172**, 551–553 (1968).

<sup>35</sup>B. J. Campbell, H. T. Stokes, D. E. Tanner, and D. M. Hatch, *J. Appl. Crystallogr.* **39**, 607–614 (2006).

<sup>36</sup>R. T. Shannon and C. T. Prewitt, *Acta Crystallogr., Sect. B* **25**, 925–946 (1969).

<sup>37</sup>R. T. Shannon, *Acta Crystallogr., Sect. A* **32**, 751–767 (1976).

<sup>38</sup>D. Pettifor, *Solid State Commun.* **51**, 31–34 (1984).

<sup>39</sup>I. Grinberg and A. Rappe, *Phase Transitions* **80**, 351–368 (2007).

<sup>40</sup>M. Weller, T. Overton, J. Rourke, and F. Armstrong, *Inorganic Chemistry* (OUP Oxford, 2014).

<sup>41</sup>F. Cheng, Z. Xia, X. Jing, and Z. Wang, *Phys. Chem. Chem. Phys.* **17**, 3689–3696 (2015).

<sup>42</sup>E. Clementi and D. L. Raimondi, *J. Chem. Phys.* **38**, 2686–2689 (1963).